scientific reports

Check for updates

OPEN

Chemical composition-driven performance evaluation model for sbs-modified asphalt using multivariate statistical

Dahai Liu[1,2], Jintao Li[3], Huaicun Guo[1,2], Kecheng Yang[1,2], Qingxia Cao[1,2], Fucheng Guo[3] & Tengfei Yao[3✉]

The performance of modified asphalt is closely related to its chemical composition. The further correlation study between chemical composition and performance gives a boost to the effective quality control of modified asphalt. The modified asphalt with a SBS modifier content of 4.5% was selected as the research object. The contents of asphaltene (As), resin (R), aromatic fraction (Ar), and saturated fraction (S) were tested using a rod-shaped thin-layer chromatography, and the succinic index ($I_{c=c}$), carbonyl index ($I_{c=o}$), and sulfoxide index ($I_{s=o}$) were determined using a fourier transform infrared spectrometer. In addition, the phase angle (θ), complex shear modulus (G^*), fatigue factor ($G^* \sin\theta$), and rutting factor ($G^*/\sin\theta$) of modified asphalt were obtained through dynamic shear rheological tests. At the same time, the basic performance indicators of SBS modified asphalt were tested. Based on the grey correlation theory, the correlation degree between various performance indicators of SBS modified asphalt and the four components was established, and the indicator factors for establishing the factor model were determined according to the magnitude of the correlation degree. Through factor analysis, a performance optimization model for modified asphalt was ultimately established. The results showed that, except for Δm, all other indicators had a good correlation with the four components. Among them, softening point (SP) had the highest correlation with As and R, while θ had the highest correlation with Ar and S. The modified asphalt indicators were reduced to two factors F_1 and F_2 through factor analysis, and the factor weights were calculated to obtain the principal component formula. Finally, the model was validated using modified asphalt with different SBS modifier dosages, and the results showed the feasibility of the model in assessing the performance of modified asphalt.

Keywords SBS modified asphalt, Chemical composition, Grey correlation analysis, Factor theory, Principal component analysis

The rapid expansion of highway infrastructure has significantly increased the utilization of polymer-modified asphalt in pavement engineering due to its enhanced performance characteristics[1]. However, the proliferation of modification manufacturers has resulted in substantial quality variations among commercial products. Effective quality control of modified asphalt has therefore become critically important in construction practices[2,3]. Empirical observations from industrial production reveal that even with identical processing parameters, batch-to-batch performance inconsistencies persist, posing challenges for material standardization[4].

As established in asphalt science, binder quality fundamentally determines pavement service life, with modified asphalt performance being intrinsically linked to base asphalt properties, polymer modifiers, and processing conditions - factors ultimately manifested in chemical composition and microstructural variations[5]. The four-component composition (saturates, aromatics, resins, and asphaltenes) serves as the molecular "molecular determinants" governing asphalt's macroscopic characteristics[6–9]. Component proportions critically influence key performance metrics including viscosity, adhesion, aging resistance, thermomechanical behavior, and rheological response[10,11,11]. Notably, SBS modification introduces polymer-aromatic interactions

during thermal processing, altering the original four-component equilibrium of base asphalt. This molecular restructuring creates measurable compositional disparities between modified asphalt and its base material[12,13].

The advent of material informatics and the accumulation of modified asphalt big data have driven increasing utilization of intelligent algorithms in deciphering microstructure-macroscopic property relationships[14,15]. This paradigm shift embraces the concept of "material genetic engineering", establishing quantitative mappings between chemical composition, microstructural features, and macroscopic performance through advanced statistical modeling and computational simulations. Such approaches enable cross-scale information integration across material development, production, and field application[16,18,18]. Ren et al.[19] used molecular dynamics simulation to develop more realistic molecular models to represent generic reclaimers, predicted the energetic, dynamic, volumetric, and structural properties of various reclaimers, and experimentally verified the adequacy of the simulations. Analyzing 1320 datasets, Eidgahee et al.[20] systematically compared artificial neural networks, ensemble methods, and genetic algorithms for dynamic modulus evaluation in hot-mix asphalt. Ghanizadeh et al.[21] developed a predictive model for the change in porosity of asphalt concrete with time in service. The predictive model was constructed based on 324 experimental data sets by combining evolutionary polynomial regression, pedagogical optimization algorithms, and multigene genetic programming. Input parameters included initial porosity, average annual air temperature, asphalt viscosity, and time. Upadhya et al.[22] A machine learning approach was used to construct a predictive model for Marshall stability and asphalt content in carbon fiber reinforced asphalt concrete using asphalt content, carbon fibers, asphalt grades, and fiber length as four parameters.

Grey correlation analysis (GCA) and factor analysis (FA) have emerged as powerful tools for investigating performance-structure relationships in complex material systems. Fan et al.[23] investigated the correlation between chemical composition and rheological properties of asphalt after aging and regeneration, and based on Gray Entropy Correlation Analysis (GECA), the correlation of the tested parameters was analyzed linearly, in which the rutting factor, creep stiffness, and creep rate showed a univariate linear relationship. Wang et al.[24] Optimized the traditional gray model by using the Particle Swarm Algorithm (PSO) and the Markov model to obtain a more accurate pavement performance evaluation model. Li et al.[25] evaluated the effect of different phases of graphene oxide on the high-temperature rheological properties of asphalt by using gray correlation method and principal component analysis, and provided a comprehensive evaluation of the high-temperature performance of composite modified asphalt. Xu et al.[26] established a new evaluation model for the aging of asphalt pavements based on artificial neural networks (ANNs) and gray relational analysis (GRA), and the viscosity values predicted by the model and the data were compared with the viscosity values predicted by the data. The viscosity values predicted by the model are consistent with the results of the data backcalculated values, indicating that the newly developed field aging model is able to accurately describe the field aging evolution of asphalt pavement. Liu et al.[27] investigated the common influencing factors among the rutting influencing factors by using the factor analysis method (FAM), and established a rutting evaluation model, which proved to have a high evaluation accuracy, indicating that the FAM is an effective rutting evaluation model indicator screening method.

In this study, the modified asphalt with a SBS modifier content of 4.5% was selected as the research object. The contents of asphaltene (As), resin (R), aromatic fraction (Ar), and saturated fraction (S) were tested using a rod-shaped thin-layer chromatography, and the succinic index (Ic=c), carbonyl index (Ic=o), and sulfoxide index (Is=o) were determined using a fourier transform infrared spectrometer. In addition, the phase angle (θ), complex shear modulus (G*), fatigue factor (G* sinθ), and rutting factor (G*/sinθ) of modified asphalt were obtained through dynamic shear rheological tests. At the same time, the basic performance indicators of SBS modified asphalt were tested. With the help of gray correlation analysis and factor theory, the relationship between the chemical compositions and macro performance of modified asphalt was studied, and the relevant evaluation model was established. Through the application of performance evaluation model, the performance quality of modified asphalt is tested, so as to provide technical support for material design and performance evaluation in the production process of modified asphalt, which can effectively guarantee the stable production quality of modified asphalt. A comprehensive performance evaluation model integrating chemical composition characteristics and performance indicators has been developed. This model not only clarifies the dominant role of key components in performance changes but also enables the quantifiable evaluation of asphalt performance. The research framework of this study is illustrated in Fig. 1.

Materials and methods
Materials
Raw materials
(1) Matrix asphalt: 90# asphalt (ZH 90#) produced by Sinopec Zhenhai Refining&Chemical Co., Ltd. was used, and all indicators meet the requirements of the specifications.

(2) SBS modifier: White granular linear SBS (styrene-butadiene-styrene block copolymer) modifier produced by Sinopec was used, with a styrene content of 31.1% (mass fraction).

SBS modified asphalt
Using ZH 90# asphalt as the base asphalt to produce modified asphalt, the modifier content is 2%, 3%, 4%, 4.5, 5%. Preparation process: First, heat the base asphalt to 180 ℃, slowly add the SBS modifier while stirring at low speed, and maintain the premix for 15 min. Then, perform high-speed shearing at 5000 rpm for 45 min (at 200 ℃), followed by aging at a constant temperature of 180 ℃ for 30 min. Finally, degas and take samples. The production of modified asphalt physical indicators are shown in Table 1.

Table 1 shows D (ductility), SP (softening point), η (viscosity), and Δm (mass change). The experimental data for modified bitumen formulations with different SBS contents (Table 1) show that under standardized
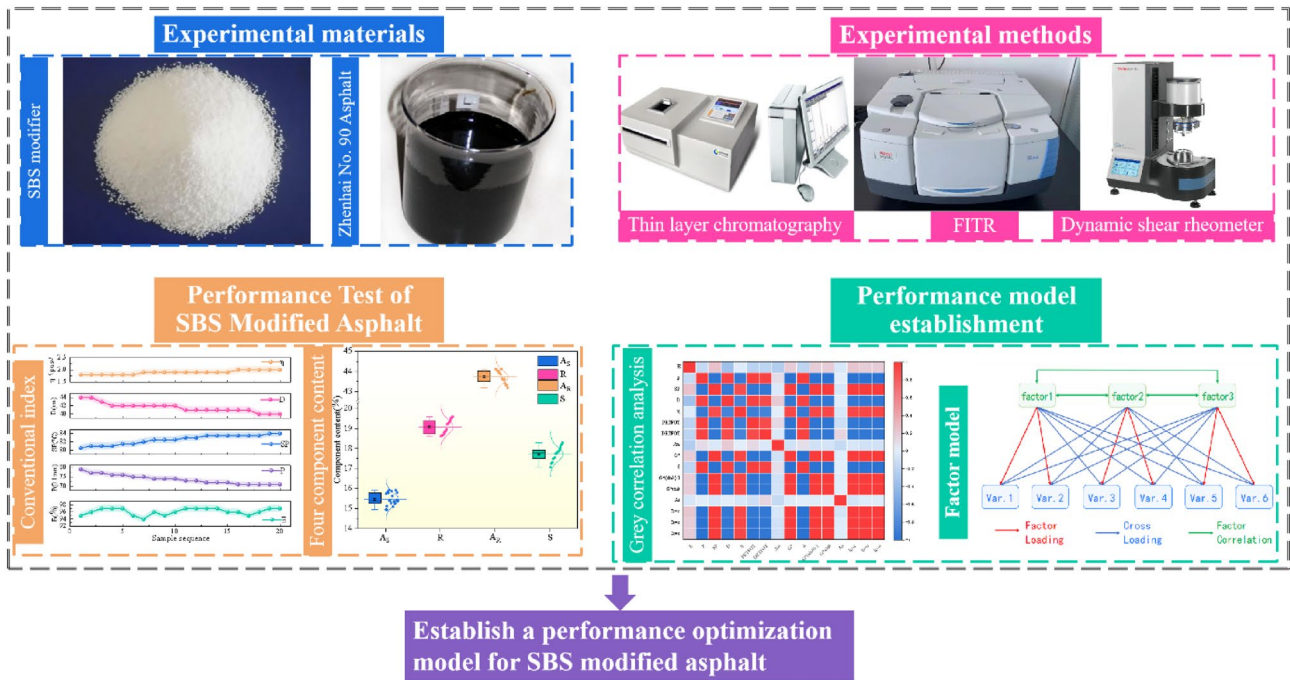
Fig. 1. The research framework of this study.

Test Item	SBS content					Technical requirement
	2%	3%	4%	4.5%	5%	
D	37	30	29.1	33	38	≥ 30 cm
SP	56.5	61.5	70	80	87	≥ 55℃
η	0.7	0.95	1.34	1.99	2.4	≤ 3.0 Pa·s
Δm	−0.3	0.01	0.01	−0.05	−0.2	± 1.0%
P/P_{RTFOT}	70	68.4	68.8	75	82	60 ~ 80 mm
D_{RTFOT}	13	13	14	23	23	≥ 20 cm
SP_d	0.5	0.3	0.4	1.6	3	≤ 2.5℃

Table 1. Basic performance parameters of SBS modified asphalt.

production conditions, the improvement of key performance parameters is concentration dependent. Specifically, 5 °C ductility (D), softening point (SP), 135 °C viscosity (η), D_{RTFOT} and storage stability (SPd) were positively correlated with SBS content. According to t JTG F40-2004 specification, the SBS I-C modified asphalt could only meet the requirements for 5℃ ductility and D_{RTFOT} when the SBS modifier content is greater than 4%. Considering that with the increase of SBS content, the segregation softening point difference may also increase, leading to the segregation risk of SBS modified asphalt. At the same time, an increase in SBS content will also cause an increase in the viscosity of modified asphalt and an increase in production costs. Therefore, the SBS modified asphalt with a modifier content of 4.5% was selected for subsequent performance testing.

Rod thin layer chromatography test

The content of modified asphalt asphaltene, resin, aromatic fraction, and saturated fraction was measured using a rod-shaped thin-layer chromatography and chromatographic analysis software[28]. The experiment used SF-2020 rod thin layer chromatography, H13 chromatography column, and neutral alumina (100–200 mesh) adsorption column. The cleaning solution consists of n-hexane (analytical grade), toluene (analytical grade), petroleum ether (60–90 ℃), benzene (chemical alcohol), and ethanol (chemical alcohol). 0.5 g asphalt was weighed and dissolved in 30 ml of n-heptane solution through continuous stirring. Then, 1 ml of the prepared sample is extracted and carefully dropped onto an activated adsorption column. The column was sequentially rinsed with elution solutions to separate four distinct fractions. The solution was dropped onto the chromatography rod and was subsequently placed in the analytical instrument for analysis and testing. Each batch of samples undergoes three parallel tests, with RSD controlled within 5% to improve testing accuracy. The main sources of error include uneven column packing density, sample loading fluctuations, solvent elution sequence deviations, and chromatographic image analysis errors. These errors are controlled through standardized operating procedures and automatic image recognition software.

Fourier infrared spectroscopy test

The infrared spectroscopy analysis of modified asphalt could effectively distinguish the presence of SBS modifier. By further analyzing the ratio of characteristic peak areas of carbonyl, sulfoxide, and butadiene at 1700 cm^{-1}, 1030 cm^{-1}, and 966 cm^{-1} to 1377 cm^{-1}, the functional group indices of carbonyl, sulfoxide, and butadiene could be quantified[29,30]. The main experimental process is to first scan the background of the crystal plate, and then heat and stir the SBS modified asphalt sample to be tested. After stirring evenly, a scraper is used to take the sample and apply it to the crystal plate. The Fourier transform infrared spectrometer is used for testing to obtain the infrared spectrum. Import the obtained modified asphalt infrared spectrum into OMINIC software for spectral processing, calculate peak areas, and sequentially read the characteristic peak areas of the infrared spectra at 1700 cm^{-1} carbonyl, 1030 cm^{-1} sulfoxide, 966 cm^{-1} butadiene, and 1377 cm^{-1} wave numbers. FTIR employs polystyrene film calibration to ensure wavenumber accuracy, background scanning to correct system noise, and OMNIC software for integral analysis of characteristic peaks (e.g., C = O, S = O, C = C, etc.), using the 1377 cm^{-1} peak as the normalization reference. Sample film thickness is consistent, with 32 scans averaged to ensure spectral stability. The primary sources of error include uneven sample film formation, sample contamination, baseline drift, and functional group changes caused by high-temperature oxidation.

The peak area of characteristic functional groups of asphalt infrared spectrum is selected for quantitative analysis, and the quantitative basis of absorption peak area is defined:

$$I_{c=c} = A_{966}/A_{1377} \tag{1}$$

$$I_{c=o} = A_{1700}/A_{1377} \tag{2}$$

$$I_{s=o} = A_{1031}/A_{1377} \tag{3}$$

In the formula, $I_{c=c}$ is the is the butadiene functional group index; $I_{c=c}$ is the carbonyl functional group index; $I_{s=c}$ is the sulfoxide functional group index; A_{96} is the absorption peak area of butadiene; A_{1700} is the peak area of carbonyl absorption peak; A_{1031} is the absorption peak area of sulfoxide group; A_{1377} is the peak area of the absorption peak at a wavelength of 1377 cm^{-1}.

Dynamic shear rheological test

Perform temperature scanning tests were used by a high-precision TA-AR1500ex rheometer. The original SBS modified asphalt and PAV(Pressurized Aging Vessel) aged asphalt were used in the experiment. The test results of the original asphalt were used to calculate the complex shear modulus G*, phase angle θ, and rutting factor G*/sinθ, while the test results of the PAV aged asphalt were used to calculate the fatigue factor G*sinθ. The instrument loading mode was set to strain control mode, with a strain level of 12%, a loading frequency of 10 rad/s, and a temperature scanning range of 58 ℃, 64 ℃, and 70 ℃. After the temperature reaches equilibrium, 20 cycles of sine wave loading were performed for each temperature, and the data from the last 10 cycles were taken to calculate the complex shear modulus and phase angle, and then calculate the rutting factor and fatigue factor.

Results and discussion

Performance test of SBS modified asphalt

Under the condition of modifier content of 4.5%±0.1%, 20 SBS modified asphalt samples were randomly produced by using different batches of ZH 90# matrix asphalt (with slightly different components) and the same production process, and the regular performance, dynamic shear rheological performance, infrared spectrum and rod thin layer chromatography were tested respectively. The 20 SBS modified asphalt samples were sorted according to the penetration degree from large to small, and numbered as 1, 2, …, 20.

Regular performance of SBS modified asphalt
As shown in Figs. 2 and 3, modified asphalt increases the softening point, increases the power viscosity and decreases the ductility as the needle penetration decreases. This is because the smaller the needle penetration, the greater the consistency of the asphalt, the harder the physical properties, the better the high temperature performance, and the higher the softening point. The flexural and tensile properties of the asphalt decrease, as evidenced by the decrease in ductility. The trend of viscosity and needle penetration is opposite, because bitumen with low needle penetration contains relatively more heavy components, becomes viscous, and the dynamic viscosity increases at 60°C[32]. From the indices of SBS modified asphalt before aging, when the difference in SBS content is small, the indices of SBS modified asphalt such as needle penetration, ductility, softening `point, viscosity and other indices are affected by the four components.

As can be seen from Fig. 3, after 85 min of short-term aging of different asphalt samples, the ductility of asphalt significantly decreased when the asphalt penetration in the sequence of asphalt samples was low, indicating that thermo-oxidative aging has a significant effect on the flexural and tensile properties of asphalt. Under the influence of thermo-oxidative aging, the light component in the asphalt was transformed into the heavy component[31].

SBS modified asphalt four-component test results
The four component contents of the SBS modified asphalt tested according to the thin layer rod chromatography are shown in Fig. 4. Figure 4(a) reflects the content distribution of the four components of SBS modified asphalt. Asphaltene, as the component with the highest molecular weight and the strongest polarity in asphalt, the asphaltene content of SBS-modified asphalt is about 15% to 16%. The saturated fraction of asphalt consists of aliphatic hydrocarbons, alkyl cyclic hydrocarbons and some alkyl aromatic hydrocarbons, etc. Most of the
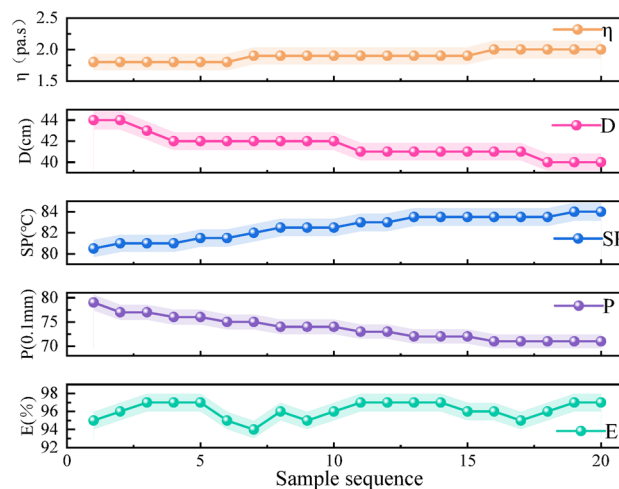
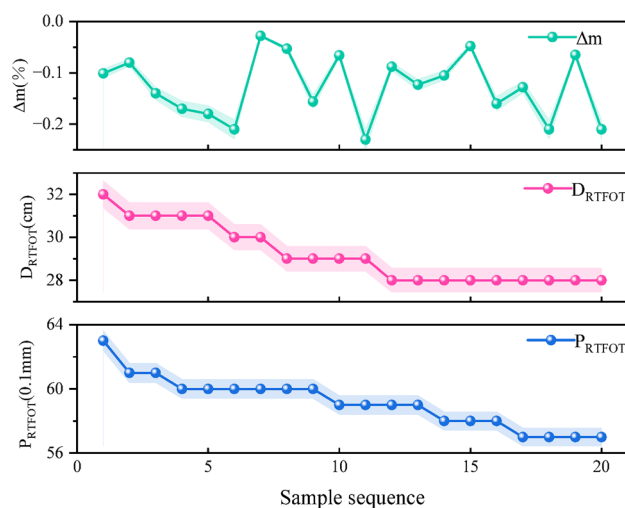**Fig. 2.** Regular indicators before aging.

Fig. 3. Indicators after Aging.

saturated fraction is non-polar thick oils with an average molecular weight between 300 and 2000. The saturated fraction of SBS-modified asphalt is roughly between 17% and 18.5%. Resins, due to their strong polarity, exhibit excellent adhesive properties in asphalt and also serve as dispersants or peptizing agents for asphaltenes. The ratio of resins to asphaltenes significantly influences the colloidal type of asphalt. In SBS-modified asphalt, the content of the resins ranges between 18% and 20%. The aromatic fraction, recognized as the naphthenic-aromatic compounds with the lowest molecular weight in asphalt, is primarily composed of non-polar carbon chains. Due to their ability to disperse asphaltenes within the asphalt matrix, aromatic fractions play a critical role in maintaining the colloidal system in a stable state. In SBS-modified asphalt, the content of the aromatic fraction ranges between 43% and 44%.

As shown in Fig. 4(b), when the penetration of asphalt gradually decreases, the corresponding asphalt colloid content gradually increases, while the content of aromatic and saturated components decreases, asphalt in the performance of the "hard" state, that is, the internal components of the change through the external performance. This is related to the role of asphalt 4 components in the asphalt colloid structure, strong polarity of high molecular weight asphaltene is the core of the asphalt colloid structure, the performance of asphalt has an important impact, while the saturated and aromatic components as the main dispersed phase, play a role in softening the colloid and the asphaltene to form micelles. It can be seen that changes in asphalt composition can directly affect the performance of asphalt, changes between components, basic physical properties of asphalt, rheological properties, etc., and the composition is usually regarded as an important bridge to analyze the potential relationship between the micro-composition and macro-properties of asphalt[27].
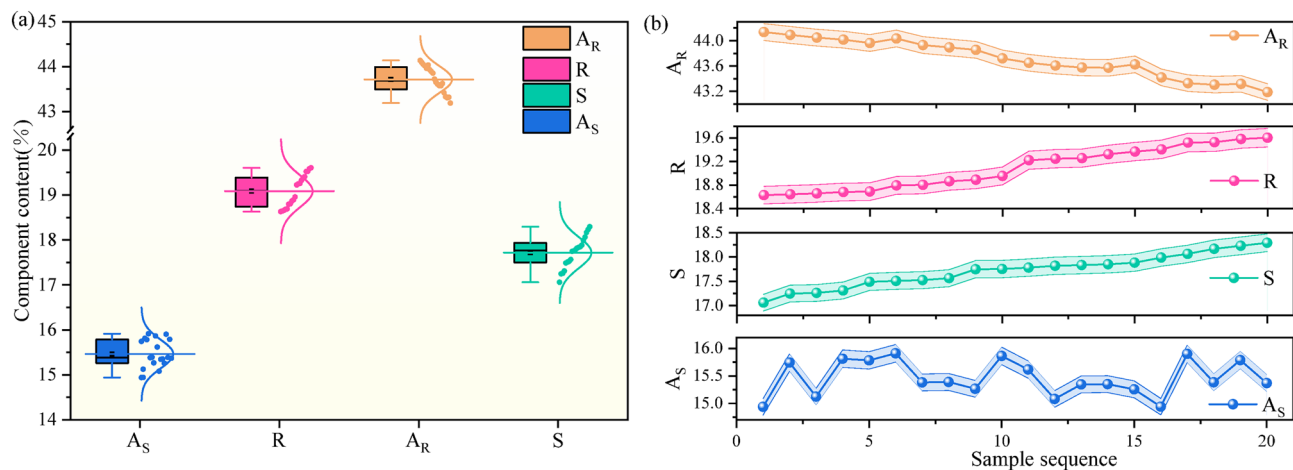
Fig. 4. Test results of four component content of SBS modified asphalt(**a**. Content distribution of four components of SBS modified asphalt, **b**. Trends in the content of the four components of SBS modified asphalt).
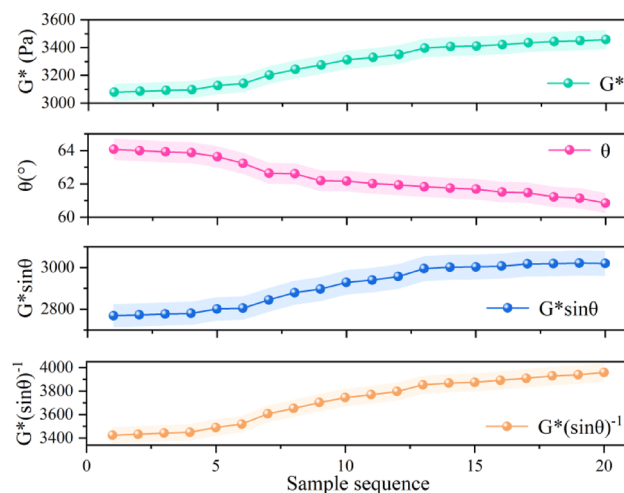

Fig. 5. Test results of rheological properties of SBS modified asphalt.

SBS modified asphalt rheological performance test results

The complex shear modulus, phase angle, rutting factor and fatigue factor of SBS modified asphalt were obtained by temperature scanning test at 64 ℃. as shown in Fig. 5.

As can be seen in Fig. 5, as the permeability of the asphalt sequence decreases, the complex shear modulus increases, the phase angle gradually decreases, and the rutting factor and fatigue factor increase. This is due to the fact that the heavy component in the composition of low permeability asphalt samples contains more asphaltenes than other samples with the same oil source, and the heavy component is less sensitive to high temperature and its high temperature stability is improved. Under high temperature conditions, the lower the energy consumption of asphalt, the lower the flow deformation and the higher the rutting resistance, so the rutting factor has been used as an index to evaluate the permanent deformation of asphalt[33]. In addition, the phase angle can be used to characterize the viscous component of the modulus under load for the same complex shear modulus. As the permeability decreases, the fatigue factor of the asphalt sequence increases and the fatigue resistance properties decrease. Therefore, to ensure the fatigue resistance of asphalt pavements, "hard" asphalt should not be blindly pursued, and the heavy fraction of asphalt should be controlled within a reasonable range.

Fourier transform infrared spectroscopy of SBS modified asphalt

The indices of carbonyl, sulfinyl and butadiene functional groups were determined by analyzing the ratios of carbonyl, sulfinyl, butadiene and 1377 cm^{-1} characteristic peak areas of the infrared spectra of SBS-modified asphalt at the wavelengths of 1700 cm^{-1}, 1030 cm^{-1} and 966 cm^{-1}. The characteristic peak areas are shown in Fig. 6.
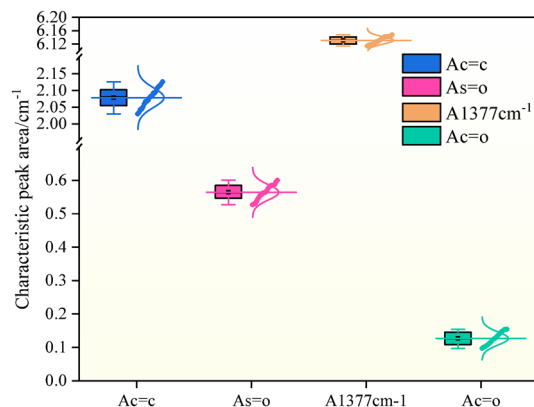
Fig. 6. Peak areas of characteristic functional groups of SBS-modified asphalt.
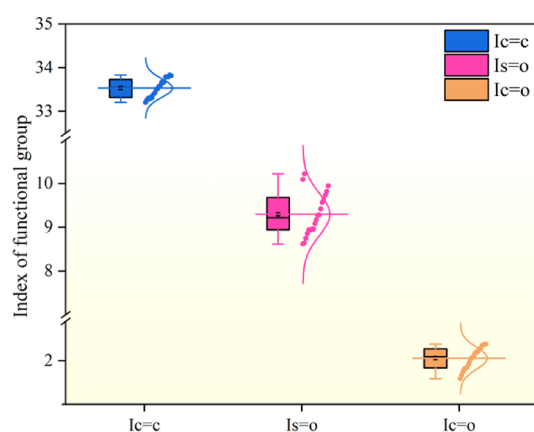

Fig. 7. Characteristic functional group index of SBS-modified asphalt.

As shown in Fig. 6, the SBS-modified asphalt has a small peak area at the sulfoxide group (S = O) and carbonyl group (C = O), indicating that the asphalt has a certain degree of oxygen absorption aging phenomenon at higher temperatures during the production and development of SBS-modified asphalt.

As can be seen from the slight variation in the magnitude of the sulfoxide and carbonyl indices in Fig. 7, the 20 asphalt samples underwent oxygen absorption aging to a similar extent due to the essentially identical matrix asphalt oil source and production process used in the production. In addition, the significant butadiene index of the SBS-modified asphalt increased as the needle penetration of the asphalt series decreased, which could be attributed to the addition of the SBS modifier to increase the viscosity of the asphalt, thus decreasing the needle penetration of the asphalt.

Gray correlation analysis of various indicators and four components

The four components of asphalt have the most direct effect on the performance of asphalt, which is called the "gene" of asphalt. In this paper, the four components of SBS-modified asphalt as a reference sequence, its performance indicators as a comparative sequence, the use of gray correlation theory, analyze the correlation between SBS-modified asphalt performance indicators and the four components, and according to the size of the correlation to determine the establishment of the factor model of the indicator factor.

The correlation degree between each index and the 4 components is calculated with the asphalt 4 components as the reference sequence. Min–Max normalization was used to preprocess performance indicators and component data. The normalization formula is as follows: The discrimination coefficient ρ was set to 0.5, which is the most commonly used empirical value in the literature. This value ensures analytical sensitivity and stability while also taking into account the ability to identify differences between indicators. And the results are shown in Table 2. The correlation analysis between the content of the four components in SBS modified asphalt and various performance evaluation indicators is shown in the Fig. 8.

$$x_i' = \frac{x_i - \min(x)}{\max(x) - \min(x)} \qquad (4)$$

Evaluation Item	Correlation degree				Rankings			
	Asphaltene	Resin	Saturation score	Aromatic	Asphaltene	Resin	Saturation score	Aromatic
SP	0.99	0.989	0.986	0.987	1	1	3	3
E	0.988	0.987	0.987	0.988	2	2	2	2
θ	0.986	0.986	0.988	0.989	3	3	1	1
$I_{c=c}$	0.984	0.984	0.98	0.981	4	4	4	4
$G^*\sin\theta$	0.976	0.975	0.971	0.972	5	5	5	5
G^*	0.968	0.968	0.964	0.965	6	6	8	8
D_{RTFOT}	0.967	0.967	0.97	0.97	7	7	6	6
P_{RTFOT}	0.967	0.967	0.969	0.969	8	8	7	7
P	0.962	0.962	0.964	0.964	9	9	9	9
$G^*/\sin\theta$	0.961	0.961	0.957	0.958	10	10	10	10
η	0.958	0.957	0.954	0.955	11	11	12	12
D	0.956	0.956	0.957	0.958	12	12	11	11
$I_{s=o}$	0.947	0.947	0.944	0.944	13	13	13	13
$I_{c=o}$	0.853	0.852	0.85	0.851	14	14	14	14
SP_d	0.72	0.72	0.719	0.721	15	15	15	15
Δm	0.523	0.523	0.523	0.523	16	16	16	16

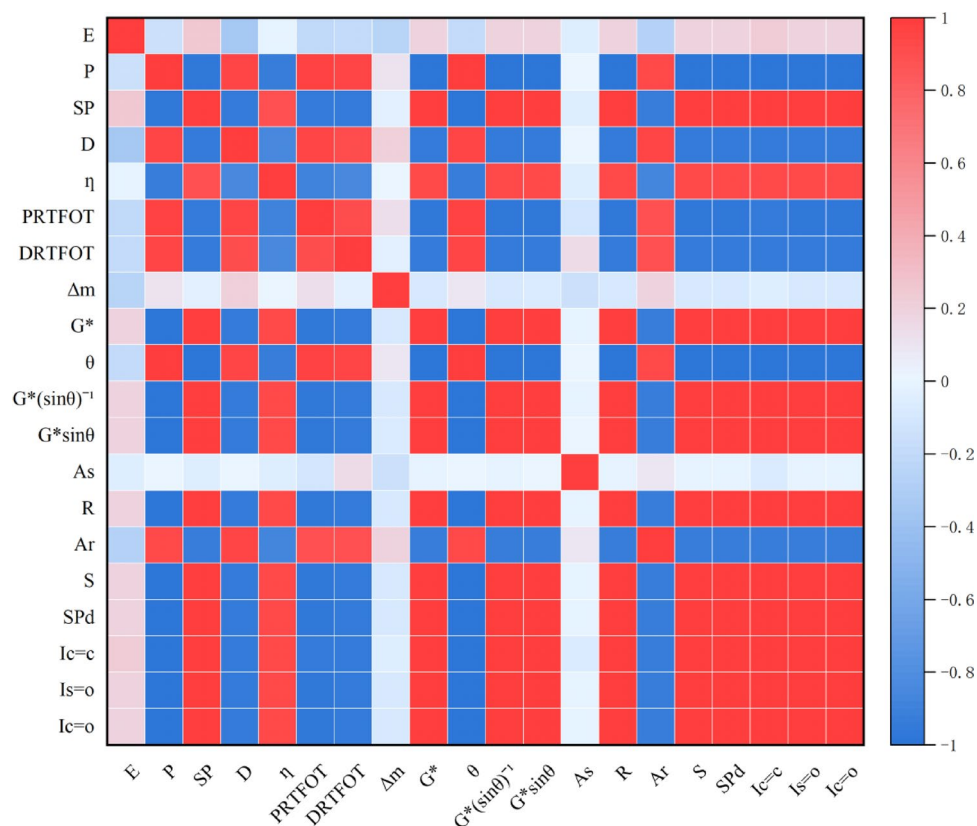**Table 2**. Correlation degree with asphaltene content as parent sequence.

Fig. 8. The correlation analysis between the content of the four components in SBS modified asphalt and various performance evaluation indicators (A_S, R, S, A_R).

As shown in Table 2, except for the mass change (Δm), the correlation of other indicators of SBS modified asphalt with the 4 components is more than 0.7, and the correlation of SBS modified asphalt indicators with asphaltenes and gums is consistent, as well as the correlation of saturated and aromatic fractions. From the correlation degree, SBS modified asphalt conventional indicators, rheological properties and aging indicators and 4 components of the correlation degree of more than 0.9, is highly correlated.
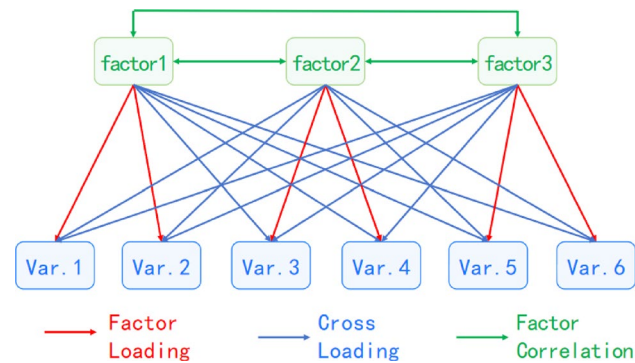
Fig. 9. Factor model.

KMO value		0.61
Bartlett sphericity test	approximate chi-square	1641.233
	df	190
	P	0.000

Table 3. KMO test and Bartlett test.

The correlation between the carbonyl index (Ic = 0), storage stability (SPd) and mass change (m) is less than 0.9, which is attributed to the fact that the carbonyl index and mass change are mainly due to the chemical reaction of the asphalt with the oxygen in the air during production and development, as well as during thermo-oxidative aging, which is influenced not only by the internal factors of the asphalt itself, but also by the external factors of the environment. Storage stability is a unique parameter that distinguishes SBS modified asphalt from base asphalt, and this index is largely influenced by the content of SBS modifier.

In summary, there is a high correlation between the four components of SBS modified asphalt and their performance indices. When the gray correlation analysis is performed, the correlation between the comparison sequence and the reference sequence is distinguished according to the correlation degree, and it is considered that when the correlation degree is greater than 0.8, the two have a large correlation. When the correlation is between 0.6 and 0.8, the two have a general correlation. When the correlation is less than 0.6, the correlation is small, and the correlation between the quality change of modified asphalt and the four components is less than 0.6, which can be ignored in the factor analysis. A high positive correlation degree indicates that as the content of the four components increases, the performance indicator also tends to increase.

Factor analysis of SBS modified asphalt

Factor analysis theory

Factor analysis is a statistical technique used in research to extract common factors from a set of variables, originally proposed by British psychologist C.E. Spearman[34]. Factor analysis identifies hidden representative factors in many variables, groups variables of the same type into a single factor, reduces the number of variables, and tests hypotheses about relationships between variables. Factor analysis is based on the idea of dimensionality reduction. Under the condition of losing no or as little information as possible from the original data, complex variables are aggregated into a few independent common factors. These common factors can reflect the most important information of the original variables. While reducing the number of variables, they also reflect the intrinsic relationship between variables. Factor analysis usually has three functions: first, it is used for factor dimensionality reduction; second, it calculates factor weights; and third, it calculates weighted factor aggregation comprehensive scores. The factor model diagram is shown in Fig. 9.

KMO inspection and Bartlett inspection

Factor analysis attempts to explain as much information as possible about all variables by a few factors. Before conducting factor analysis on the system, KMO and Bartlett's sphericity tests should be performed first to determine whether the system indicators are suitable for factor analysis. The usual criterion for determining the KMO value is 0.6. Values greater than 0.6 indicate suitability for factor analysis, while values less than 0.6 indicate unsuitability for factor analysis. Also, the corresponding p-value of Bartlett's test less than 0.05 indicates that the factor analysis is suitable. Although KMO > 0.6, it is in the critical range. The main reasons for this low value may include the following two aspects: there is strong correlation between variables, leading to potential multicollinearity; and some variables have weak discriminative power or redundant information. Table 3 shows the results of KMO and Bartlett's test of sphericity for 19 variables, including conventional indices, four components, rheological properties, and functional group index of infrared spectra for 20 groups of modified bitumen samples.

As can be seen from Table 3, the KMO value of the sample is 0.61, which may be low due to insufficient sample size. However, the significance p-value of the Bartlett's sphericity test is 0.000, which still meets the conditions for factor analysis, indicating that it is significant at this level. The null hypothesis is rejected and there is a correlation between the variables with a medium correlation level, so the factor analysis is valid.

Variance interpretation table
The interpretation of the total variance is showed in Table 4. When performing factor analysis, components with eigenvalues greater than 1.0 are selected. The 1 st and 2nd components in the table have eigenvalues greater than 1.0 and a cumulative variance explained of 91.607%, which is greater than 60%. Two factors may contain more than 90% of the information in the original data.

Factor load coefficient table
The transformed factor loading coefficients is showed in Table 5, which reflect the degree of agreement between the extracted factors and the different indicators. From the table, it can be seen that the common degree of the storage stability separation (SPd) indicator is the smallest, which is 0.152, while the common degree of all other indicators is greater than 0.85. From the magnitude of loading coefficients of factor 1, the correlation between storage stability separation and elasticity recovery rate is the smallest, while the correlation coefficients between these two indicators and factor 2 are 0.366 and 0.939, which are ranked in the top three, respectively. Therefore, although the common degree of the storage stability separation indicators is only 0.152, their importance to factor 2 was not discarded when building the factor model. S has a loading of −0.966 on Factor 1, meaning that as the content of saturated components increases, the overall performance level represented by this factor decreases.

Based on the high loadings observed in Table 5, Factor 1 (F1) is predominantly associated with indicators related to high-temperature stiffness and compositional consistency (e.g., complex shear modulus, rutting factor, softening point, and asphaltene/resin content). In contrast, Factor 2 (F2) is strongly linked to elastic recovery and storage stability, which are more directly influenced by the SBS polymer network. Thus, while mathematical abstractions, F1 and F2 can be interpreted as representing the 'Base Asphalt Rigidity Factor' and the 'Polymer Modification Factor', respectively.

Component matrix analysis
Table 6 presents a matrix of components designed to illustrate the factor score coefficients (principal component loadings) included in each component, which are used to calculate component scores and derive the principal component formula.Each term in Eq. (5) corresponds to an indicator in Table 6, with the coefficient representing Factor 1; Each term in Eq. (6) also corresponds to an indicator in Table 6, with the coefficient representing Factor 2.

Ingredients	Rotation forward difference interpretation rate			Rate of variance interpretation after rotation		
	Characteristic root	Variance interpretation rate (%)	Cumulative variance interpretation rate (%)	Characteristic root	Variance interpretation rate (%)	Cumulative variance interpretation rate (%)
1	16.365	86.133	86.133	1567.605	82.506	82.506
2	1.04	5.474	91.607	172.932	9.102	91.607
3	0.985	5.184	96.792			
4	0.236	1.24	98.032			
5	0.156	0.823	98.855			
6	0.077	0.405	99.26			
7	0.072	0.381	99.641			
8	0.022	0.113	99.754			
9	0.018	0.095	99.85			
10	0.012	0.063	99.913			
11	0.006	0.034	99.947			
12	0.006	0.03	99.977			
13	0.002	0.011	99.988			
14	0.001	0.006	99.994			
15	0.001	0.004	99.998			
16		0.002	100			
17			100			
18			100			
19			100			

Table 4. Variance interpretation table.

Indicator Name	Factor load coefficient after rotation		Common degree (common factor variance)
	Factor 1	Factor 2	
A_s	0.979	0.177	0.989
R	0.976	0.19	0.989
S	−0.966	−0.231	0.987
A_r	−0.963	−0.17	0.957
P	−0.964	−0.201	0.97
D	−0.872	−0.379	0.904
SP	0.959	0.237	0.976
η	0.952	−0.018	0.906
SP_d	0.134	0.366	0.152
E	0.026	0.939	0.882
P_{RTFOT}	−0.916	−0.249	0.9
D_{RTFOT}	−0.943	−0.171	0.919
$I_{c=c}$	0.97	0.224	0.99
$I_{c=o}$	0.976	0.177	0.984
$I_{s=o}$	0.973	0.193	0.983
θ	−0.98	−0.139	0.98
G^*	0.974	0.178	0.981
$G^*(\sin\theta)^{-1}$	0.978	0.172	0.986
$G^*\sin\theta$	0.967	0.186	0.971

Table 5. .Factor load Coefficients.

Indicator Name	Ingredients		Indicator Name	Ingredients	
	Factor 1	Factor 2		Factor 1	Factor 2
A_s	0.067	−0.02	P_{RTFOT}	−0.047	−0.058
R	0.064	−0.007	D_{RTFOT}	−0.064	0.018
S	−0.055	−0.032	$I_{c=c}$	0.057	0.025
A_r	−0.066	0.023	$I_{c=o}$	0.066	−0.019
P	−0.06	−0.006	$I_{s=o}$	0.063	−0.004
D	−0.018	−0.186	θ	−0.074	0.055
SP	0.053	0.039	G^*	0.0022	−0.0018
η	0.101	−0.194	$G^*(\sin\theta)^{-1}$	0.0027	−0.0024
SP_d	−0.055	0.031	$G^*\sin\theta$	−0.0012	−0.001
E	−0.017	0.086			

Table 6. Composition matrix.

$$
\begin{aligned}
F_1 = &\; 0.067 \times A_s + 0.064 \times R - 0.055 \times S - 0.066 \times A_r - 0.06 \times P \\
&- 0.018 \times D + 0.053 \times SP + 0.101 \times \eta - 0.055 \times SP_d - 0.017 \times E - 0.047 \times P_{\mathrm{RTFOT}} \\
&- 0.064 \times D_{\mathrm{RTFOT}} + 0.057 \times I_{c=c} + 0.066 \times I_{c=o} + 0.063 \times I_{s=o} - 0.074 \times \theta + 0.0022 \times G^* \\
&+ 0.0027 \times G^*\sin\theta^{-1} - 0.0012 \times G^*\sin\theta
\end{aligned}
\tag{5}
$$

$$
\begin{aligned}
F_2 = &\; -0.02 \times A_s - 0.007 \times R - 0.032 \times S + 0.023 \times A_r - 0.006 \times P - 0.186 \times D + 0.039 \times SP \\
&- 0.194 \times \eta + 0.312 \times SP_d + 0.086 \times E - 0.058 \times P_{\mathrm{RTFOT}} + 0.018 \times D_{\mathrm{RTFOT}} + 0.025 \times I_{c=c} - 0.019 \times I_{c=o} \\
&- 0.004 \times I_{s=o} + 0.055 \times \theta - 0.0018 \times G^* - 0.0024 \times G^*\sin\theta^{-1} - 0.001 \times G^*\sin\theta
\end{aligned}
\tag{6}
$$

Factor weight analysis
From the above, we can obtain the comprehensive factor F calculation formula (5):

$$
F = 0.90064 \times F_1 + 0.09936 \times F_2
\tag{7}
$$

Model validation
To verify the applicability of the model of Eq. (6), two modified asphalt samples were prepared using ZH90# base asphalt with SBS modifier added according to the ratios of 4.5%(A) and 4.3%(B) using the same production process and were tested separately, and the results are shown in Table 8. The test results were substituted into Eq. (4) and Eq. (5) to calculate the factors F_1 and F_2, respectively, and then the composite factor F was calculated

Indicator Name	Explanation of variance after rotation/%	Cumulative variance interpretation rate after rotation/%	Weight/%
Factor 1(F_1)	82.506	82.506	90.064
Factor 2(F_1)	9.101	91.607	9.936

Table 7. Factor weight analysis.

Sample	Test results of asphalt sample index								
	$I_{c=o}$	A_r	S	$I_{s=o}$	P	D_{RTFOT}	D	η	SP	G^*
4.5%	0.025	44.03	16.12	0.103	71	28	40	2.0	84	3158
4.3%	0.018	45.72	15.80	0.090	75	30	42	1.8	81.5	3442

Sample	Test results of asphalt sample index								
	E	SP_d	$I_{c=c}$	θ	$G^*(\sin\theta)^{-1}$	P_{RTFOT}	A_s	R	$G^*\sin\theta$
4.5%	97	1	0.344	60.85	3959	57	16.03	19.71	2820
4.3%	95	0	0.336	63.23	3519	60	16.66	19.60	3586

Table 8. SBS modified asphalt verification sample (A, B) indicators.

according to Eq. (6). The composite factors of the validation samples (A, B) and the test samples (1,2,…, 20) for the composite factor F are shown in Table 9.

By calculating the composite factor F scores of 20 groups of test samples and 2 groups of validation samples, it can be seen that the scores of validation samples A and B are between the maximum and minimum of the scores of test samples, which proves that there is no bias in the results of the model calculations and the model results are reliable. The scores of asphalt samples A and B are 1.057 and 0.965, respectively, and the score of asphalt sample A is higher than that of asphalt sample B, indicating that asphalt sample A is better than that of asphalt sample B. From the results of the indicators of the two types of asphalt, the softening point, viscosity, and rutting resistance coefficient of asphalt A are slightly higher than that of asphalt B. The penetration, elongation, shear modulus and fatigue coefficient are slightly lower than that of asphalt B, which indicates that asphalt A has good high temperature performance and fatigue performance, and higher fatigue performance. The inferior ductility may cause the low temperature performance of bitumen B to be better than that of bitumen A. The difference between the factor analysis scores of bitumen A and bitumen B also reflects the difference in the consistency of their performance, which can prove that the model obtained by factor analysis is feasible.

According to the test samples of 20 sets of data, SBS-modified asphalt comprehensive factor scores generally obey the asphalt penetration degree, the higher the ranking of the more backward law. Through the front of the asphalt 4-component effect on various properties concluded that: with the decline of asphalt sequence needle penetration, the asphalt in the group component increases, the viscosity of asphalt increases, the modified asphalt softening point and power viscosity increases, the ductility decreases, the complex shear modulus increases, rutting coefficient and fatigue coefficient increases, the phase angle gradually decreases. The overall high temperature performance, fatigue performance and water stability performance of asphalt improved. The low temperature performance decreased, and the asphalt with high value showed better performance in terms of comprehensive performance indicators.

Factor contribution analysis

The composite factor F can be seen as the sum of the two parts, as shown in Eq. (8):

$$F = 0.90064 \sum \varepsilon_i f_i + 0.09936 \sum \lambda_i f_i \qquad (8)$$

Among them, ε_i and λ_i represent the magnitude of factor 1 and factor 2 of I indicators, respectively, as shown in Table 6; fi represents the detection results of I indicators. As shown in Eq. (7), the contribution of each indicator to the composite factor is composed of $\varepsilon_i f_i$ and $\lambda_i f_i$. Due to the large difference in the value and unit of each asphalt indicator, ε_i and λ_i cannot directly evaluate the contribution rate of each indicator to F only from the magnitude of coefficient 1 and coefficient 2 of each indicator in Table 6. In order to facilitate the observation and analysis of the contribution of the indices to F, Eq. (7) is treated as follows:

$\varepsilon_i f_i = \varepsilon_i \overline{f_{in} f_i} / \lambda_i \overline{f_{in} f_i} / \overline{f_{in}}$, Among them $\overline{f_{in}}$ denotes the mean of the I-th indicator for n samples. Order $\varepsilon_i \overline{f_{in}}$、$\lambda_i \overline{f_{in}}$, Respectively ε'_i、λ'_i, then Eq. (7) becomes Eq. (9):

$$F = 0.90064 \sum \varepsilon'_i f_i / \overline{f_{in}} + 0.9936 \sum \lambda'_i f_i / \overline{f_{in}} \qquad (9)$$

For the 20 samples in this study, ε'_i、λ'_i the results are shown in Table 10.

From the analysis of the factor weights in Table 7, it can be seen that the weight of Factor 1 is about 10 times that of Factor 2, so the ranking of the indicators and the size of the factors in Table 10 are based on ε'_i. Since the $fi/\overline{f_{in}}$ value of the same asphalt is close to 1, the sizes of ε'_i and λ'_i basically reflect the degree of

Asphalt sample	A	B	1	2	3	4	5	6	7	8	9
Comprehensive score	1.071	0.987	−1.549	−1.459	−1.248	0.247	−1.127	−0.589	−0.686	0.403	0.711
Rankings	5	6	22	21	20	14	19	17	18	12	9
Asphalt sample	10	11	12	13	14	15	16	17	18	19	20
Comprehensive score	−0.098	0.680	0.338	−0.120	0.781	0.857	1.234	1.141	1.378	1.332	0.546
Rankings	15	10	13	16	8	7	3	4	1	2	11

Table 9. Comprehensive factor F score of SBS modified asphalt factor model.

Indicator Name	Ingredients				Indicator Name	Ingredients			
	ε'_i	Rankings	λ'_i	Rankings		ε'_i	Rankings	λ'_i	Rankings
$G^*(\sin\theta)^{-1}$	10.689	1	−9.502	19	D	−0.720	11	−7.440	18
G^*	7.895	2	−5.684	17	S	−0.887	12	−0.516	14
SP	4.452	3	3.276	3	E	−1.678	13	8.342	1
R	1.261	4	−0.138	10	D_{RTFOT}	−1.792	14	0.504	5
A_s	1.074	5	−0.321	11	P_{RTFOT}	−2.679	15	−3.306	16
η	0.200	6	−0.388	12	A_r	−2.906	16	1.013	4
$I_{c=c}$	0.020	7	0.009	7	$G^*\sin\theta$	−3.384	17	−2.820	15
$I_{s=o}$	0.002	8	−0.00048	9	P	−4.260	18	−0.426	13
$I_{c=o}$	0.006	9	−0.00041	8	θ	−4.503	19	3.347	2
SP_d	−0.055	10	0.031	6					

Table 10. ε'_i, λ'_i results Statistics.

contribution of the indicators to the *F* value. The positive and negative values in the table reflect the direction of the contribution, and the size of the value reflects the degree of contribution. From Table 10, it can be seen that rutting coefficient, complex shear modulus, softening point, gel content and asphaltene content are the main positive contribution indicators; phase angle, penetration, fatigue coefficient, aromatic content, penetration after aging at 25℃, ductility after aging at 5℃, elastic recovery rate, saturation content and ductility are the negative contribution indicators.

Practical Application and Workflow: The F-factor model serves as a rapid evaluation tool for quality control. In practice, manufacturers first establish a database by calculating the F-factor for numerous SBS-modified asphalt batches that have passed performance verification. Once this database is established, for subsequent production batches, manufacturers primarily need to measure the four-component composition of the base asphalt and verify the SBS dosage. The F-factor for the new batch can then be calculated and compared against the acceptable range of F-factors in the qualified database. If F' falls outside this range, it indicates potential performance deviation, allowing proactive adjustment of the production process before conducting comprehensive performance testing. This model saves time and resources by screening for potential nonconforming products using a small number of rapid chemical tests.

ConclusionS

(1) The four-component composition of SBS modified asphalt exhibits a significant correlation with its macroscopic performance. Asphalt with lower penetration demonstrates higher proportions of heavy components, such as asphaltene and resin, whereas the aromatic and saturated fractions are relatively reduced. Consequently, this compositional shift results in elevated softening points, increased dynamic viscosity, reduced ductility, and greater consistency in the asphalt. Due to the lower temperature sensitivity of the heavy components, asphalt rich in these constituents exhibits enhanced complex shear modulus, rutting factor, and fatigue factor, alongside a diminished phase angle, thereby improving resistance to deformation. However, such compositions may compromise fatigue resistance. To ensure balanced pavement performance, the content of heavy components in asphalt should be optimized through comprehensive consideration of multiple performance criteria.

(2) With the exception of the mass change (Δm), all other performance indicators of SBS-modified asphalt exhibit high correlation degrees (>0.8) with the four-component composition (asphaltenes, resins, aromatics, and saturates). In contrast, the correlation degree between Δm and the four components is notably lower (<0.6). This discrepancy arises from the combined influence of intrinsic and extrinsic factors: during production and thermal-oxidative aging processes, volatilization of light components and chemical transformations alter the asphalt composition. Such changes lead to mass variations that are not solely governed by the four-component equilibrium, thereby reducing the observed correlation.

(3) The performance index of modified asphalt was simplified into two factors, F_1 and F_2, by using factor analysis, and a comprehensive evaluation model of $F = 0.90064 \times F_1 + 0.09936 \times F_2$ was established according to the magnitude of its weights. Through verification, the model is feasible in evaluating the performance of modified asphalt.

(4) By optimizing the modified asphalt factor model, the contribution of each index of the modified asphalt to the overall score of the model was compared. The rutting coefficient, complex shear modulus, softening point, gum content, and asphalt content were obtained as the main positively correlated indexes; phase angle, penetration, fatigue coefficient, aromatic content, penetration after aging at 25℃, elongation after aging at 5℃, elastic recovery, saturation, and elongation were negatively correlated indexes.

(5) Although this study established a performance evaluation model for SBS-modified asphalt based on chemical composition, it still has limitations. Only a single oil source and a fixed type of SBS modifier were used. Asphalt components vary significantly depending on the crude oil source, and the modification mechanisms of star-shaped SBS and linear SBS differ, limiting the model's universality. While focusing on a 4.5% SBS content is representative of engineering applications, it ignores the nonlinear effects of dosage changes on the "component-performance" relationship.Therefore, this model only demonstrates the feasibility of this approach. However, in practical applications, it should be recalibrated using local materials to ensure effective implementation.

(6) This study primarily focuses on establishing a robust "composition-property" relationship under a fixed and commonly used SBS content (4.5%), which represents a critical first step in quality control during production. We recognize that extending the model to cover a broader range of SBS contents (2%−5%) is essential for wider applicability. Given the limitations of this study, future research could be deepened in the following directions: combining molecular dynamics simulations with atomic force microscopy techniques to reveal the interaction mechanisms at the interfaces of SBS-modified asphalt components; establishing a cross-scale correlation model linking molecular structure, phase transition evolution, and macroscopic properties; constructing a standardized database covering SBS-modified asphalt from different oil sources and types; Integrating machine learning techniques (e.g., graph neural networks GNN) to handle high-dimensional nonlinear relationships, thereby enhancing the model's generalization capability.

Data availability

All data generated or analyzed during this study are included in this published article.

References

1. Jin, D. et al. Laboratory performance and field demonstration of asphalt overlay with recycled rubber and tire fabric fiber[J]. *Constr. Build. Mater. Aug.* **9**, 438 (2024).
2. Liu, Z. & Wang, Z. Development of terminal blend rubber and SBS modified asphalt: A case study. *Constr. Build. Mater.* **334**, 127459 (2022).
3. Chen, M. et al. A review of phase structure of SBS modified asphalt: affecting factors, analytical methods, phase models and improvements. *Constr Build. Mater*, **294**,123610 (2021).
4. Jin, D. et al. Resurface of rubber modified asphalt mixture with stress absorbing membrane interlayer: from laboratory to field application. *Constr. Build. Mater.* **441**, (000), 13 (2024).
5. Zhang, Z. et al. Thermosetting resin modified asphalt: A comprehensive review. *Traffic Transp. Eng. Engl. Ed.* **10**, 1001–1036 (2023).
6. Li, G. et al. Effect of genes on rheological properties of asphalt binders. *Fuel* **365**, 131324 (2024).
7. Xing, C. et al. Review and prospect of genetic characteristics of asphalt mixture based on material genome method. *China J. Highw Transp.* **33**, 76–90 (2020).
8. Gao, M. et al. Molecular dynamics study on the compatibility of asphalt and rubber powder with different component contents. *Acs Omega.* **7**, 36157–36164 (2022).
9. Yang, C. et al. Investigation of physicochemical and rheological properties of SARA components separated from bitumen. *Constr. Build. Mater.* **235**, 1–13 (2020).
10. Xu, J. et al. Microstructural, chemical and rheological evaluation on oxidative aging effect of SBS polymer modified asphalt. *Constr. Build. Mater.* **267**, 121028 (2021).
11. Sultana, S. & Bhasin, A. Effect of chemical composition on rheology and mechanical properties of asphalt binder. *Constr. Build. Mater.* **72**, 293–300 (2014).
12. Airey, G. D. Rheological properties of styrene butadiene styrene polymer modified road bitumens. *Fuel* **82**, 1709–1719 (2003).
13. Zhang, H. et al. Examining the rheological and adhesion performance of asphalt: insights into the influence of SARA components. *Case Stud. Constr. Mater.* **21**, e03427 (2024).
14. Liu, Z. Y. et al. Review and prospects of performance enhancement of asphalt mixtures based on material informatics[J]. *China J. Highw Transp.* **37**, 98–120 (2024).
15. Li, C. & Zheng, K. Methods, progresses, and opportunities of materials informatics. *InfoMat* **5**, e12425 (2023).
16. Liu, J. et al. Optimizing asphalt mix design through predicting effective asphalt content and absorbed asphalt content using machine learning. *Constr. Build. Mater.* **325**, 12660718 (2022).
17. Zhang, K. et al. Enhancing Understanding of asphalt mixture dynamic modulus prediction through interpretable machine learning method. *Adv. Eng. Inf.* **65**, 10311119 (2025).
18. Yuan, W. L. et al. Materials-genome approach to energetic materials. *Acc. Mater. Res.* **2**, 692–696 (2021).
19. Ren, S. et al. Chemical characterizations and molecular dynamics simulations on different rejuvenators for aged bitumen recycling. *Fuel* **324**,124550 (2022).
20. Rezazadeh Eidgahee, D. et al. Data-driven Estimation models of asphalt mixtures dynamic modulus using ANN, GP and combinatorial GMDH approaches. *NEURAL COMPUT. APPL.* **34**, 17289–17314 (2022).
21. Ghanizadeh, A. R. et al. A formulation for asphalt concrete air void during service life by adopting a hybrid evolutionary polynomial regression and multi-gene genetic programming. *Sci. Rep.* **14**, 1325423 (2024).
22. Upadhya, A. et al. Modelling and prediction of binder content using latest intelligent machine learning algorithms in carbon fiber reinforced asphalt concrete. *Alexandria Eng. J.* **65**, 131–149 (2023).
23. Fan, G. et al. Correlation analysis of chemical components and rheological properties of asphalt after aging and rejuvenation. *J. Mater. Civ. Eng.* **34**, 04022303 (2022).
24. Wenping, W. & Zheng, M. Integrity analysis and inverse Deng's grey relational analysis model. *J. Southeast. Univ. (English Edition)* **39**, 248–255 (2023).
25. Li, B. et al. Effect of graphene oxide in different phases on the high temperature rheological properties of asphalt based on grey relational and principal component analysis. *Constr. Build. Mater.* **362**, 129714 (2023).

26. Xu, P. et al. Field aging characterization of asphalt pavement based on the artificial neural networks and Gray relational analysis. *J. Mater. Civ. Eng.* **35**, 04023188 (2023).

27. Gang, L. et al. Rutting influencing factors and prediction model for asphalt pavements based on the factor analysis method. *J. Southeast. Univ. (English Edition)* **37**, 421–428 (2021).

28. Makowska, M. & Pellinen, T. Thin layer chromatography performed in stages to identify the presence of aromatic like fraction in chosen bitumen modifiers. *Journal of Traffic and Transportation Engineering (English Edition).* **8**, 453-466.32 (2021).

29. Ji, H. et al. Adhesion mechanism of warm-mixed recycled SBS modified asphalt binder: surface free energy, microstructure and chemical compositions. *Case Stud. Constr. Mater.* **19**, e02426 (2023).

30. Zhang, H. et al. Contributions of fourier-transform infrared spectroscopy technologies to the research of asphalt materials: A comprehensive review. *Fuel* **371**, 13207831 (2024).

31. Zhang, Z. et al. Preparation and properties of a novel high-viscosity modified bitumen. *Constr Build. Mater* **344**,128183 (2022).

32. Nie, Y. et al. Evaluation of ageing behaviors of asphalt binders using FTIR tests. *Int. J. Pavement Res. Technol.* **14**, 615–624 (2021).

33. Mei, L. et al. Effect of microstructure of recycled asphalt on rheological properties. *J. HUAZHONG U SCI-MED.* **.47**, 121–126 (2019).

34. Tian, P. et al. Characteristics' relation model of asphalt pavement performance based on factor analysis. *Int. J. Pavement Res. Technol.* **11**, 1–12 (2018).

35. Jiang, Q., Liu, W. & Wu, S. Analysis on factors affecting moisture stability of steel slag asphalt concrete using grey correlation method[J]. *J. Clean. Prod.* **397**, 136490 (2023).

36. Kyriazos, T. & Poga, M. Dealing with multicollinearity in factor analysis: the problem, detections, and solutions[J]. *Open. J. Stat.* **13**(3), 404–424 (2023).

37. Jin, D. et al. Evaluation of lab performance of stamp sand and acrylonitrile styrene acrylate waste composites without asphalt as road surface materials. *Constr. Build. Mater. Jul.* **4**, 338 (2022).

38. Jin, D. et al. Waste cathode-ray-tube glass powder modified asphalt materials: Preparation and characterization. *J. Clean. Prod.* **314**, 127949 (2021).

39. Jin, D. et al. Performance of rubber modified asphalt mixture with tire-derived aggregate subgrade. *Constr. Build. Mater.* **449** (000), 17 (2024).

Acknowledgements

Author contributions

writing—original draft preparation, Dahai Liu; writing—review and editing, Jintao Li; Conceptualization, Huaicun Guo; methodology, Fucheng Guo; supervision, Tengfei Yao; project administration, Kecheng Yang; investigation, Qingxia Cao; resources, Qingxia Cao.

Funding

Declarations

Competing interests

The authors declare no competing interests.

Additional information

Correspondence and requests for materials should be addressed to T.Y.

Reprints and permissions information is available at www.nature.com/reprints.

Publisher's note Springer Nature remains neutral with regard to jurisdictional claims in published maps and institutional affiliations.